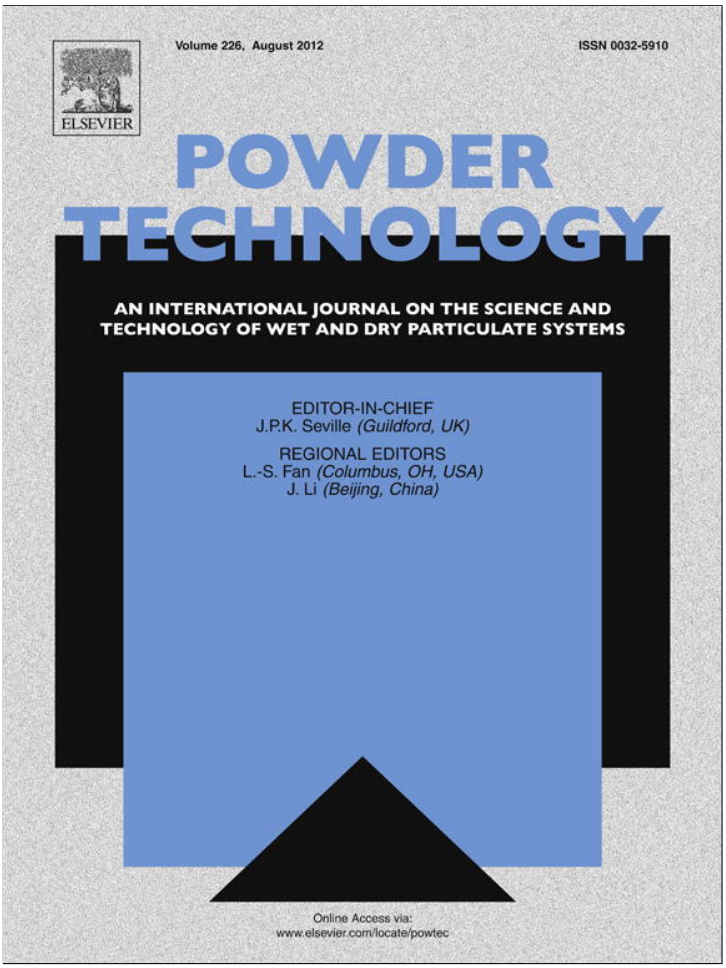

Powder Technology 226 (2012) 107–113

Contents lists available at SciVerse ScienceDirect

Powder Technology

journal homepage: www.elsevier.com/locate/powtec

Effect of particle size distribution and calcium aluminate cement on the rheological behaviour of all-alumina refractory castables

Abílio P. Silva [a], Ana M. Segadães [b,*], Deesy G. Pinto [a], Luiz A. Oliveira [c], Tessaleno C. Devezas [a]

[a] University of Beira Interior, Dept. Electromechanical Eng. (CAST), 6200-001 Covilhã, Portugal
[b] University of Aveiro, Dept. Ceramics and Glass Eng. (CICECO), 3810-193 Aveiro, Portugal
[c] University of Beira Interior, Dept. Civil Eng. and Architecture (CMADE), 6200-001 Covilhã, Portugal

ARTICLE INFO

Article history:
Received 8 February 2012
Received in revised form 5 April 2012
Accepted 14 April 2012
Available online 23 April 2012

Keywords:
Particle size distribution
Rheology
Calcium aluminate cement
Refractory castables
Design of experiments

ABSTRACT

Previous works based on statistical design of experiments (DoE) defined a model all-alumina self-flow refractory castable (SFRC) with optimized particle size distribution for simultaneous high flowability index (FI) and superior post-sintering performance.
This work compares the SFRC rheological behaviour and setting time with those of alternative all-alumina castables with different *Andreasen* aggregate particle size distribution modulus, and of the equivalent castables containing calcium aluminate cement. The model castable showed Bingham behaviour with low yield stress, viscosity and thixotropy, guaranteeing easier casting and less wear in the casting and/or projection equipment. However, as the coarse particle fraction increases, the castable flow tends to be non-linear and changes from Bingham to Herschel–Bulkley. The cement containing castables quickly loose flowability despite the applied shear.
This work confirmed previous conclusions based on FI measurements and demonstrates the adequacy of the use of FI values in the calculation of FI response surface by DoE.

1. Introduction

Over the last decades, unshaped hydraulic bond refractory products have gained increasing popularity due to easy installation in all kinds of high temperature applications. Refractory castables for monolithic linings are supplied as premixed dry powder blends to which the necessary kneading water is added for in situ mixing and casting. The paste-like mixture must flow and then harden in place to yield a dense refractory lining. Water is necessary for the development of the hydraulic bonds and as vehicle for casting. However, excessive added water promotes coarse particle segregation and, upon drying, leaves behind undesirable porosity, which hinders some of the most important properties of the sintered refractory lining, namely, mechanical strength and corrosion resistance. Nevertheless, and although used in rather small amount (typically between 3 and 8% in conventional refractory castables), water is a key ingredient in refractory castables. Thus, research efforts have been directed at reducing the kneading water requirement, while keeping the desired rheological characteristics of the fresh castable (workability) and the thermomechanical performance of the sintered lining [1–7].

Given that the added water first fills the voids between solid particles, the obvious way to reduce the water requirement is to maximise the powders packing density, i.e. to have an *Andreasen* particle size distribution modulus, q, near 0.37 (q is the slope of the line tangent to the cumulative particle size distribution curve plotted on a logarithmic scale). However, maximum particle packing translates into minimum flowability and the ideal *Andreasen* q values should be near 0.22, which corresponds to a reduced interference between coarse particles (i.e. higher maximum paste thickness, MPT) [3,6,8–11].

With limited water content, the flowability role has to be played by a matrix of fine powders, frequently called glidants, that increases the distance between coarse particles and reduces their interference, thus being responsible for the paste-like behaviour of the fresh castable [6,8,9,11]. Although the presence of the aggregate (coarse particles) hinders the flowability of the fresh castable, it improves the sintered castable mechanical strength and reduces firing shrinkage, contributing also to the reduction of the castable cost [10]. Also, given that the water volume increases dramatically upon vaporization, it ensures a safe lining permeability level since severe damage can occur during the castable first heat-up if no escape routes are provided for water vapour. In this event, the pressure build-up inside the lining can surpass the lining mechanical strength with the consequent risk of lining destruction and personal injury.

Workability can be improved by external vibration but when this is not possible or advisable, self-flow refractory castables (SFRC) are used. A SFRC "works" as a suspension of powders in which the fine matrix is the flow medium that envelops the aggregate particles, fills in the voids between them and suspends them, thus promoting higher

* Corresponding author. Tel.: +351 234 370 236; fax: +351 234 370 204.
E-mail address: segadaes@ua.pt (A.M. Segadães).

0032-5910/$ – see front matter © 2012 Elsevier B.V. All rights reserved.
doi:10.1016/j.powtec.2012.04.028

flowability index (FI). Earlier works [6,8–10] report on studies on the optimization of the particle size composition of a model castable (100% alumina) for maximum fresh paste flowability and sintered body mechanical strength, using statistical design of experiments [12,13] and calculation of mathematical models to describe the various properties (response surfaces). Those works showed that the fresh castable FI is more sensitive to the increase in the specific surface area than to the increase in added water content [14], as the presence of a higher amount of fine particles separates the aggregate particles further apart (higher MPT values) and reduces the interference between them [6]. On the other hand, it is also fundamental to guarantee a minimum aggregate content, whose self-weight also promotes the castable's flowability, leading to a final gap-sized particle size distribution (PSD) [11]. As a result, the ideal matrix content for castable self-flow (80%<FI<130%) was set at 47.5 wt.%, corresponding to an overall PSD with a gap between ~40 and 250 μm, specific surface area (SSA) above 2.466 m^2/g and a MPT value between 100 and 150 μm.

Within the aggregate fraction, the combination of particle sizes was also found to affect the final castables FI, and a new simplex experiment design was established to calculate the FI response surface as a function of the aggregate particle sizes [6]. However, the statistical validation of the full mathematical model returned low determination coefficients ($R^2 = 0.76$, $R_{adj} = 0.56$) and the function test ($F_{value} > F_{test}$) did not satisfy the mathematical requirements [12]. This result might raise some doubts about the adequacy of the FI test, in all its simplicity, to characterize the flowability behaviour of these materials. Nevertheless, for routine use in production, a flowability test must be robust and simple and it is envisaged that rheology tests might provide deeper insight and eventually validate the flowability index results.

Just like in other cement-based materials, after mixing with water a structure develops between particles within the fresh paste. That structure needs to be ruptured (particles must rearrange to move past each other) for the paste to flow during casting. In other words, the fresh paste shows a finite yield stress τ_0 (Pa), whose value mostly depends on the strength of the bonds established while at rest, and then flows with a constant plastic viscosity η (Pa.s). These are the typical constants that describe a Bingham rheological behaviour [15–18], which can be described by a flow curve written as in Eq. (1):

$$\tau = \tau_0 + \eta\dot{\gamma}. \quad (1)$$

In Eq. (1), τ (Pa) is the shear stress at the applied shear strain rate $\dot{\gamma}$ (s^{-1}). Bingham flow behaviour is a special case of a more general type of flow usually referred to as the Herschel–Bulkley behaviour and described by Eq. (2):

$$\tau = \tau_0 + K\dot{\gamma}^n. \quad (2)$$

In Eq. (2) K and n are constants, characteristic of the material, and this equation describes the non-linearity of the flow. When $n = 1$, the two equations become identical; if $n > 1$, as is frequently the case of concentrated suspensions, the material has a shear thickening or dilatant behaviour (the flow becomes increasingly more difficult as the applied shear strain rate increases).

In practice, similar flow curves can be obtained in fresh paste viscosity tests using a conventional rotational viscometer, which records the torque, T (N.mm), induced by the applied rotation speed, N (min^{-1}), as expressed in Eqs. (3) and (4) for Bingham and Herschel–Bulkley behaviours, respectively:

$$T = g + hN \quad (3)$$

$$T = g + aN^n. \quad (4)$$

In Eq. (3), g and h are constants, characteristic of the material, obviously related to yield stress and plastic viscosity, respectively: in the straight-line plot of T versus N, g (T axis intercept) is proportional to the yield stress and h (straight-line slope) is proportional to plastic viscosity. The graphical representation of Eq. (4) returns a power-law curve with a non-zero intercept. All numerical parameters (g, h, a, n) can be obtained by a fitting procedure (e.g. least squares) of experimental data.

Rheology tests can also be used to ascertain if the material's viscosity is, indeed, constant or, on the contrary, changes with time under a constant applied shear rate (inelasticity).

The other advantage of rheology tests is that flow curves can be recorded from rest up to a specified shear rate and then back to rest, enabling the measurement of thixotropy by the hysteresis observed between the two flow curves.

1.1. The cement addition

The construction of monolithic refractory linings relies on a bond system frequently based on calcium aluminate cement (CAC) that sets via hydration reactions at ambient temperature. Once installed and set, these refractories are dried and fired to develop ceramic bonds. However, the presence of CAC (or lime) in the ceramic matrix leads to poor high-temperature properties. Consequently, aluminate cement contents have been steadily decreased and alternative lime- or cement-free systems have been developed, often based on transitional aluminas such as γ- or ρ-Al_2O_3 [4,5].

Besides the corresponding water demand reduction and the improvement of mechanical strength at high temperature and of abrasion, corrosion and creep resistance, lower cement content also means longer working time for in situ application. However, the use of cement seems to be needed to guarantee that the castable sets with the adequate dried mechanical strength for the first service. Recent work [7] compared the thermomechanical performance of the model self-flow castable (100% alumina) with that of an equivalent castable with added CAC. With significantly longer setting time but lower dried strength, the all-alumina castable presented lower porosity, higher mechanical strength and uncompromised thermal shock resistance, turning out to be a valuable alternative when fast drying or rough green handling can be avoided.

The observed differences in setting time and workability justify, once again, a more detailed investigation of the rheological behaviour of cement containing castables.

To this purpose, the present work compares the model all-alumina self-flow castable with optimized particle size composition [6], with alternative all-alumina castables with different *Andreasen* aggregate particle size distribution modulus, and with the corresponding castables containing 0.5 and 1% calcium aluminate cement, in terms of fresh paste rheological behaviour and setting time.

2. Experimental

Tabular (T60) and reactive (CT3000SG) commercial aluminas (Almatis) were used as raw materials. The aggregate was prepared by combining three coarse size classes (0.2–0.6 mm, 0.5–1 mm, 1–3 mm). The matrix was prepared by combining the CT3000SG alumina with two other fine size classes (<63 μm and <25 μm) obtained from the commercial <0.2 mm size class.

Earlier works on design of experiments, carried out with the *STATISTICA* (data analysis software system, version 8.0, www.statsoft.com) and based on {3,2} augmented centroid simplex lattices [12,13], showed that the ideal matrix composition was 60 wt.% CT3000SG and 20 wt.% of each of the other size classes (<25 μm and <63 μm) [6], which was kept constant throughout this work, and that the required minimum matrix content for castable self-flow was 47.5% [6]. Also the ideal aggregate composition for maximum FI was found to be 10 wt.% [0.5–1 mm] and 45 wt.% of each of the other size classes (0.2–0.6 mm and 1–3 mm), corresponding to a PSD *Andreasen* modulus $q = 0.17$ [6]. This optimized all-alumina full castable is designated by MA.

For comparison purposes, three other all-alumina castables were prepared with aggregate PSD with *Andreasen* modulus of 0.22, 0.37 and 0.30, which correspond to maximum flowability, maximum particle packing density and an intermediate condition (A22, A37 and A30, respectively). The calculation of the amounts of the various size fractions was performed with the free software *EMMA* (Elkem Materials Mix Analyzer, Version 3.4.1.119, www.materials.elkem.com), as a function of the desired modulus, q [8–10].

For the cement containing castables, based on MA composition, the calcium aluminate cement CA25 (Almatis) was used. Given the similarity of particle sizes, the added cement content (0.5 and 1 wt.%) was compensated by the corresponding reduction in the amount of CT3000SG alumina. Table 1 shows the size composition of all the mixtures (without CAC: MA, A22, A30, and A37; with CAC: MAC05 and MAC1).

Powders in the selected proportions were mixed with water (28 mg/m^2 surface area, constant) in a mortar-blender (Tecnotest, 5 l) using citric acid (0.36 mg/m^2 surface area) as deffloculant, as described in the Portuguese Patent 103432 (2008) [19].

Fresh pastes were characterized in terms of Flowability Index (FI, ASTM C230 Standard) and setting time, using an adaptation of Vicat's needle test (EN 196-3 Standard). This consisted in carrying out flowability tests every 60 min, in ambient air (19 °C, 42% relative humidity) and under drying oven conditions (40 °C, 17.5% relative humidity), and recording both the spreading of the paste and the volume of existing hardened cake, until complete hardening.

Fresh pastes were also characterized at ambient temperature (~22 °C) in terms of rheological behaviour using a mortar rheometer (Viskomat NT), in which the paste drags the impeller blades as the cylindrical sample holder rotates (applied rotation speed, N), the resulting torque (T) being measured by a transducer. Two different test profiles were used, namely "step speed" and "dwell speed".

In the "step speed" profile the rotation speed is adjusted to increase stepwise with time, from zero to the stipulated maximum (20, 60, 100 and 120 rpm for castables without cement; 20, 40 and 60 rpm for castables with cement) and then reversed with the same steps back to zero. To guarantee that measured torque is an equilibrium value at each rotation speed, this speed is kept constant at each step for ~2 min before progressing to the next step. This allows the construction of equilibrium flow curves for a better determination of plastic viscosity and yield stress related coefficients (h and g, respectively).

In the "dwell speed" profile the rotation speed of the sample holder is set at a constant value (100 rpm for castables without cement and 60 rpm for castables with cement) for a long period of time (60 min). Every 2 min the speed is brought to zero and then back to the originally set value. In these variable speed periods, flow curves (T vs. N) can be constructed. This "dwell speed" profile is specially designed to evaluate how the rheological behaviour changes with time.

3. Results and discussion

3.1. Influence of the aggregate PSD in the castable flowability

Fig. 1 shows the calculated flowability index surfaces (constant FI contour plots) of matrix [8] and aggregate [6], which were used to select the corresponding ideal particle size combinations for best compromise between fresh paste flowability and sintered castable performance (highlighted in the diagrams). In terms of PSD modulus, the ideal aggregate has a q value of 0.17. Also marked on Fig. 1(b) are the aggregate size compositions with particle size distribution modulus for maximum flowability (q = 0.22), maximum particle packing density (q = 0.37) and an intermediate condition (q = 0.30).

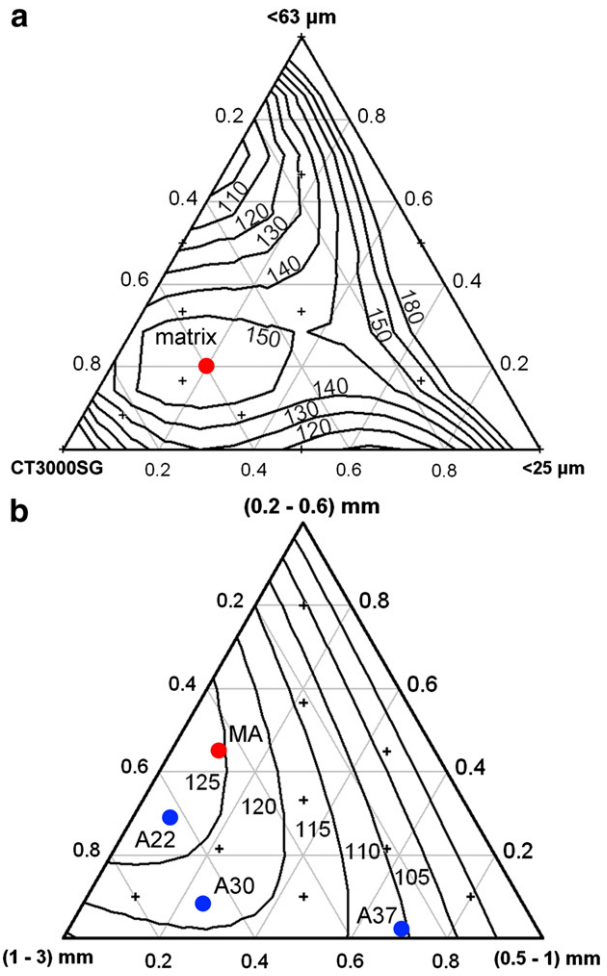

Fig. 1. Predicted FI [%] constant contour plot as a function of particle size composition: (a) matrix [8], and (b) aggregate [6]. The various mixtures studied in this work are marked in the diagrams (see Table 1 for detailed compositions).

Table 1
Particle size composition (weight %) of the castable mixtures.

Mixtures	Matrix				Aggregate		
	CA25	CT3000SG	<25 µm	<63 µm	0.2–0.6 mm	0.5–1 mm	1–3 mm
MA	0	28.5	9.5	9.5	23.63	5.25	23.63
A22	0	28.5	9.5	9.5	15.125	4.25	33.125
A30	0	28.5	9.5	9.5	4.25	13.25	35.00
A37	0	28.5	9.5	9.5	1.00	36.5	15.0
MAC05	0.5	28.0	9.5	9 .5	23.63	5.23	23.63
MAC1	1.0	27.5	9.5	9.5	23.63	5.25	23.63

Fig. 1(b) immediately shows that the aggregate PSD determined on the basis of the *Andreasen* modulus validates the FI test results: mixture A22 lies right in the centre of the highest FI region, mixture A37 lies well away from that area and mixture A30 lies in between the other two. Fig. 1 also shows that the fraction of larger aggregate particles increases from A22 to A37 and, given that the matrix content remains constant, it is expected that interference between coarser particles will increase in the same way and might induce non-linear shear thickening flow. The changes in the full castables (47.5% matrix + 52.5% aggregate) PSD can be best compared in Fig. 2, which shows the corresponding cumulative particle size distributions. The requirement of a gap-sized distribution (discontinuity in the PSD) for high flowability [11] can be clearly observed, both for the aggregate and the full castable.

Rheology tests with the "step speed" profile were carried out with the four all-alumina castables fresh pastes. Using the experimental values of torque, T, and rotation speed, N, obtained in each test, a linear regression analysis was performed to calculate the parameters, g and h, in Eq. (2) [15]. The results are given in Table 2 and suggest,

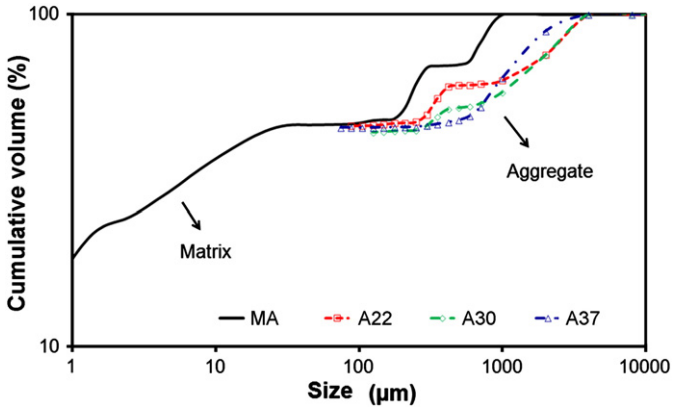

Fig. 2. Cumulative particle size distributions of all-alumina castables MA, A22, A30 and A37 (aggregate q = 0.17, 0.22, 0.30 and 0.37, respectively).

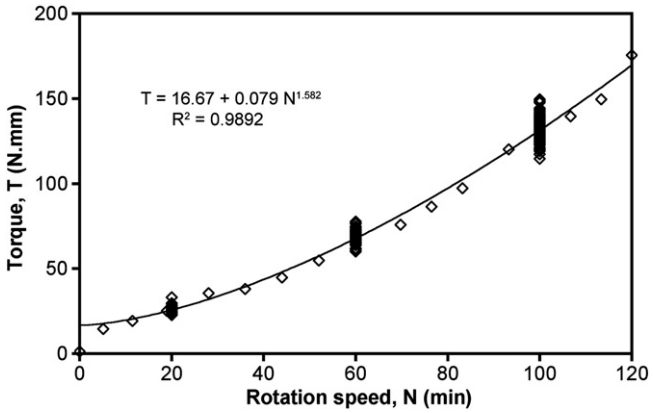

Fig. 3. Herschel–Bulkley flow curve of castable A37 (aggregate q = 0.37).

with reasonable confidence, that castables MA, A22 and A30 follow a Bingham type flow behaviour.

The negative yield stress obtained for A37, whose aggregate PSD was calculated for maximum particle packing, cannot be simply attributed to uncertainty associated with measurement (in the order of 2 N.mm) and might be the result of a high degree of non-linearity, suggesting that the flow behaviour of this mixture is of the Herschel–Bulkley type, rather than simple Bingham. Fig. 3 shows the flow curve and the corresponding fitting equation, confirming the Herschel–Bulkley behaviour described by Eq. (4).

Although the flow curves are for the full castable (matrix + aggregate), there might be some dependency between the Bingham parameters and the aggregate PSD modulus. Fig. 4 shows that approximate linear relationships exist between any of the parameters g and h, and the aggregate modulus q. Fig. 4(a) shows that the increase in aggregate PSD modulus causes a significant yield stress reduction, suggesting better particle packing, but castable A37 should not be included in this conclusion (negative g). Fig. 4(b) shows that the plastic viscosity parameter h increases with the aggregate PSD modulus: as particle packing gets denser, particle interference gets higher and flow gets more difficult. Although approximate, this tendency justifies an investigation of a possible dependence of the rheological parameters g and h with time, which can be extracted from "dwell speed" profile tests and is represented in Fig. 5.

Firstly, it can be observed that the castables hierarchy is essentially the same as in Fig. 4. However, Fig. 5(a) shows that the yield stress parameter, g, for both A30 and A37 is erratic and tends to be negative, confirming the already mentioned non-linear flow behaviour of A37, and suggesting that this is also the behaviour of A30. The other two castables (MA and A22) show a slight tendency to yield stress reduction with time.

Fig. 5(b) shows that, in general and for the observation period considered (60 min), the plastic viscosity does not change significantly with time. Again, castables A30 and A37 show an erratic behaviour. It is also interesting to note that the steadiest behaviour is observed for the model castable MA and for the castable A22, with aggregate PSD optimized for higher flowability. Of these two, MA presents the lowest viscosity h, and A22 the lowest yield stress g. From a practical application point of view, these rheological observations can be very important, given that the existence of yield stress and viscosity minima guarantee easier casting and less wear in the casting and/or projection equipment.

Data from "step speed" profile rheology tests can also be used to access the possible structural network recovery (thixotropic structural build up), as illustrated by the curves in Fig. 6. This figure shows that the thixotropic behaviour gets stronger (larger hysteresis loop) as the aggregate PSD modulus increases and is especially important for the castables A30 (q = 0.30) and A37 (q = 0.37).

This analysis of the rheology test results clearly shows the effect of the aggregate PSD modulus on the rheological behaviour of the fresh castables. Moreover, it validates the particle size optimization carried out using the DoE methodology for simultaneous fresh paste high

Table 2
Bingham flow (T = g + hN) parameters of all-alumina castables.

Mixtures	Aggregate PSD modulus, q	Yield stress, g (N.mm)	Plastic viscosity, h (N.mm.min)	R^2
MA	0.17	8.243	0.364	0.991
A22	0.22	2.590	0.620	0.994
A30	0.30	1.294	1.127	0.989
A37	0.37	−4.919	1.426	0.983

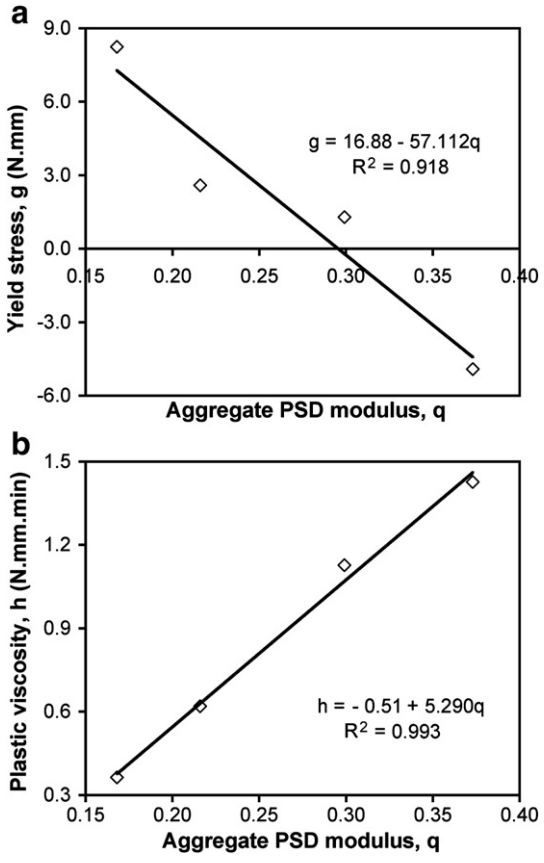

Fig. 4. Effect of aggregate PSD modulus on Bingham flow parameters: (a) yield stress g, and (b) plastic viscosity h.

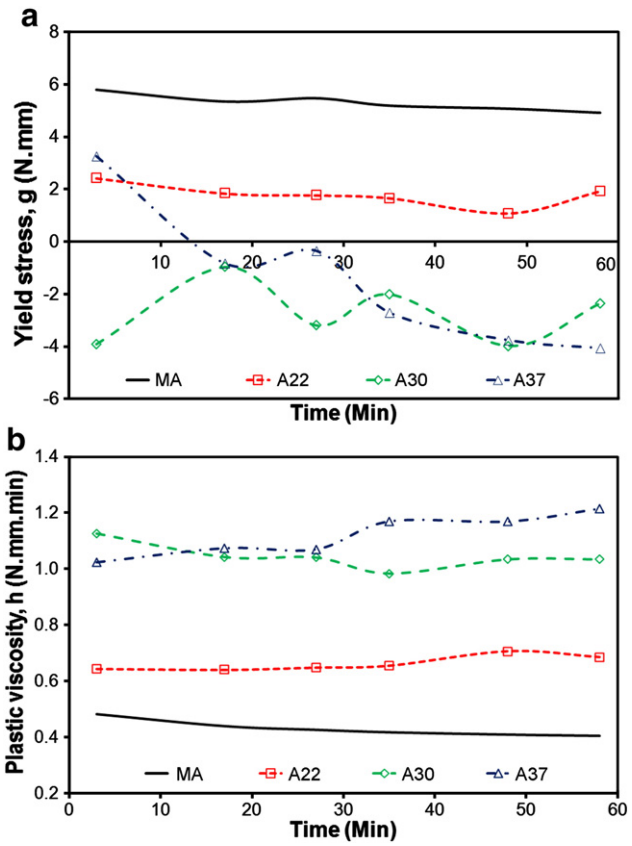

Fig. 5. Variation of Bingham flow (T = g + hN) parameters with testing time, for castables MA, A22, A30 and A37 (aggregate q = 0.17, 0.22, 0.30 and 0.37, respectively): (a) yield stress g, and (b) plastic viscosity h.

flowabilty and post-sintering performance, of which castable MA is the final result. This certainly demonstrates the adequacy of the FI test, in all its simplicity, to characterize the flowability behaviour of these materials and of the use of FI test results in the calculation of the corresponding property response surfaces such as those represented in Fig. 1.

3.2. Influence of CAC addition

Previous work carried out to compare the properties of dried and sintered bodies produced with MA and MAC1, with 1% CAC [7], showed that the presence of CAC significantly shortens the setting time, but no significant differences were observed in the expansion behaviour of the dried castables and both dried and sintered bodies reached similar densities.

However, important differences were observed in apparent (open) porosity, for which the composition with 1% CAC presents higher values (~22% higher), as a result of the formation sequence of the various calcium aluminate hydrates.

Also, the dried flexural strength was found to be much better (twice the value) for the composition MAC1, which suggest that the aluminium oxide hydrates provide a weaker bonding system, as compared to calcium aluminate hydrates. However, upon sintering, the composition without cement (and less open pores) showed a flexural strength 23% higher than that with cement [7].

As mentioned before, the presence of CAC and the consequent formation of calcium aluminate hydrates cause significant changes in the fresh paste behaviour, namely in setting time and workability. The setting time of fresh castables is usually determined with a Vicat's apparatus, which, in the case of castables without cement, raises some difficulties. Cement containing castables usually show a widespread hardening (volume hardening) whereas fresh pastes without cement start to harden from the exposed surface inwards and the interior remains liquid for a comparatively long time. Immediately after casting, a lustrous skin can be observed at the cast surface and when the Vicat's needle is pressed against the thin surface layer, the inside paste oozes out through the needle-made hole, rendering the interpretation of the test result rather difficult.

Therefore, Vicat's needle tests were replaced by a series of flowability tests in ambient air (19 °C; 42% relative humidity) and under drying oven conditions (40 °C; 17.5% relative humidity). Fig. 7 illustrates, for MA in ambient air, the aspect of the residual radial spreading (151.67 mm) and hardened cake volume (43.5 cm^3) obtained after 12 h rest inside the flowability test mould.

The results obtained in this way are presented in Fig. 8, which shows that the time needed for full consolidation gets shorter as the temperature increases, as is usually the case. Under ambient conditions the paste without CAC takes 48 h to harden, whereas at 40 °C hardening is complete within 6 h. However, after 24 h at 50 °C and

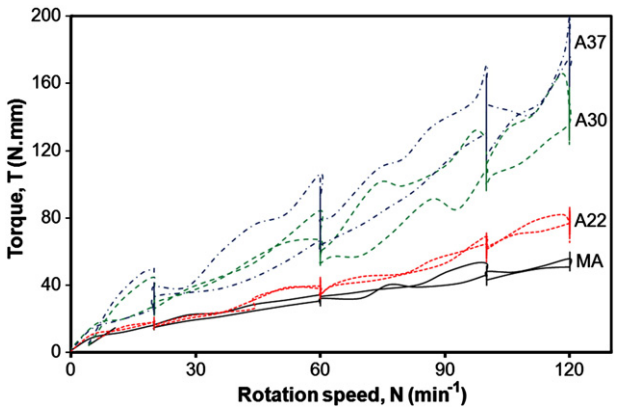

Fig. 6. Flow curves of all-alumina castables MA, A22, A30 and A37 (aggregate q = 0.17, 0.22, 0.30 and 0.37, respectively), showing the thixotropy hysteresis loop.

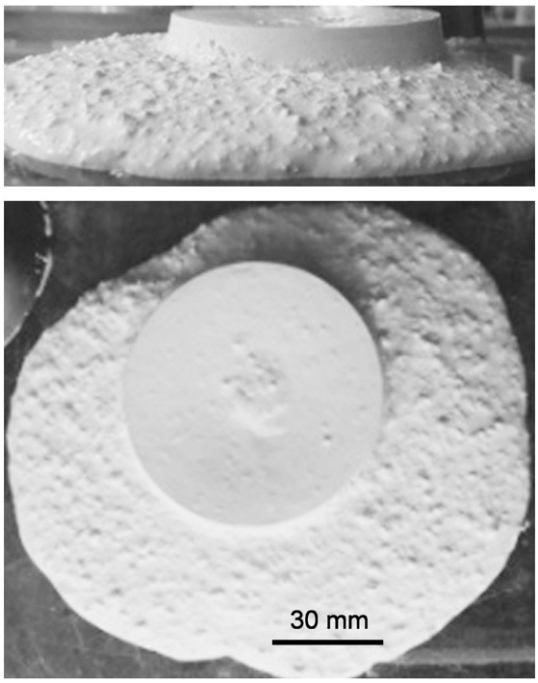

Fig. 7. Aspect of the residual radial spreading and hardened cake volume obtained for MA after 12 h rest inside the flowability test mould in ambient air. Hardening was complete after 48 h.

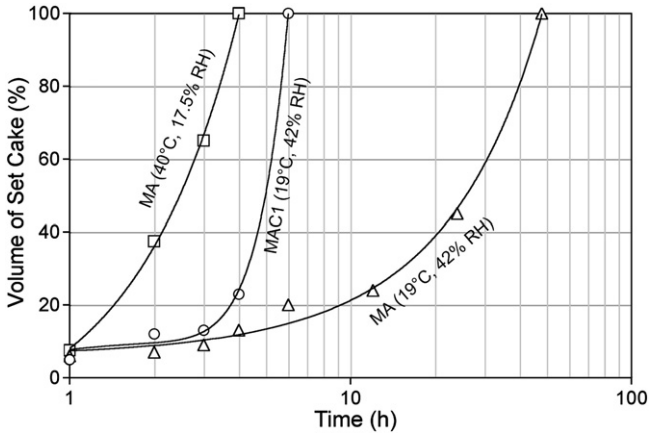

Fig. 8. Effect of setting conditions (temperature and humidity) on the volume of hardened cake obtained for MA (no cement) and MAC1 (1% CAC).

water saturated atmosphere (sample enclosed in a sealed plastic bag containing a water beaker), MA still showed no signs of hardening, not even skin formation. The corresponding MAC1 paste hardens in less than 6 h in air and less than 1 h at higher temperature.

In other words, refractory castables without cement clearly show better workability, although a longer setting time might, for some applications, be regarded as a disadvantage. In such cases, hardening can be speeded up by a rise in temperature.

It is important to notice that hardening of MA seems to be very much dependent on the exposed (drying) surface, i.e., on the surface area/volume ratio of the setting mould, confirming that a different setting mechanism is at work in the absence of calcium aluminate cement.

To further explore the absence of volume hardening, the castables workability was followed in a comparative study of the rheological behaviour of compositions without cement (MA) and with 0.5 and 1% CA cement (MAC05 and MAC1).

Fig. 9 shows the flow curves obtained using a 60 min "dwell speed" testing profile. The reference composition MA (no cement), tested at 100 rpm, requires an initial homogenizing step (30 s) to break the structure that develops since mixing. Afterwards, the flow resistance gradually decreases and after 1 h gets reduced to 75% of the initial homogenization value. At this point, the castable paste still presents high flowability, meaning that there is good workability for at least 1 h after mixing.

The composition containing 1% AC, tested at 60 rpm, shows a steep increase in resistance to flow and, after 17 min, exceeds the viscometer maximum torque. The composition containing 0.5% CAC showed a steady increase in flow resistance and, at the end of the test (60 min), a 55% increase relative to the initial resistance value could be observed.

Thus, the structure that develops during setting is certainly different when CAC is present. Without CAC, the structure within the fresh paste can be broken and re-formed almost indefinitely whereas, with CAC, a permanent structure progressively forms and gets stronger, requiring increasing torque to be broken.

Fig. 10 shows the flow curves obtained using a "step speed" testing profile, after an initial homogenizing step at 20 rpm. Again, it is clear that the hydration of the CAC and the associated volume hardening causes a steep increase in the paste flow resistance.

4. Conclusions

This work was aimed at throwing some light into the reliability of the measurements of flowability index of self-flow refractory castables and at their interpretation through rheology tests. To this purpose, an extensive comparison is made of the casting and setting behaviour of a model all-alumina SFRC with particle size distribution optimized for simultaneous fresh paste high flowability and post-sintered performance (MA), with those of alternative all-alumina castables with different *Andreasen* aggregate particle size distribution modulus (A22, A 30 and A37), and of the equivalent castables containing 0.5 and 1 wt.% calcium aluminate cement (MAC05 and MAC1).

The results obtained in rheology tests of the all-alumina castables confirmed previous conclusions based on FI measurements and showed that, as the coarse particle fraction increases, the castable flow tends to be non-linear and changes from Bingham to Herschel–Bulkley. The model castable MA, with an aggregate PSD modulus $q = 0.17$, showed a Bingham behaviour with the lowest thixotropy and plastic viscosity, and reduced yield stress. From a practical application point of view, these rheological observations can be very important, given that the existence of yield stress and viscosity minima guarantee easier casting and less wear in the casting and/or projection equipment.

Comparison between the optimized castable MA and the equivalent castables with calcium aluminate cement (CAC) showed that the presence of CAC significantly shortens the setting time and that MA is more sensitive to drying conditions (the setting time drops from 48 to 6 h, when temperature rises from 19 to 40 °C) and also to the exposed (drying) surface area/volume ratio of the setting mould, confirming the absence of the volume hardening mechanism.

The rheology results obtained demonstrate that MA shows better workability as a fresh paste, which retains its flowability as long as there is an applied shear; on the contrary, the equivalent castables with cement quickly loose their fresh paste flowability despite the applied shear.

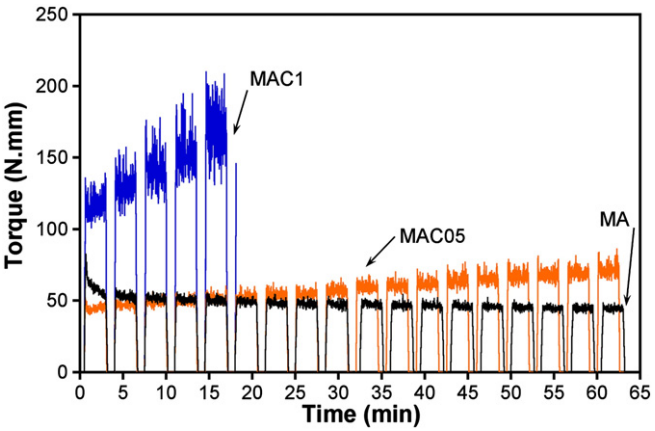

Fig. 9. Fresh paste flow curves obtained in "dwell speed" testing profile for MA (no cement), MAC05 (0.5% CAC) and MAC1 (1% CAC).

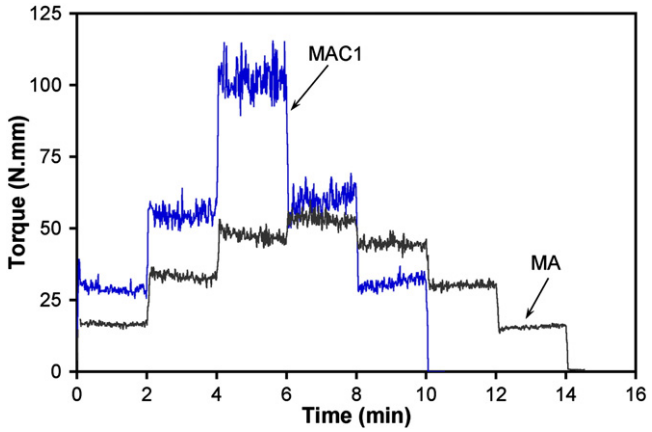

Fig. 10. Fresh paste flow curves obtained in "step speed" testing profile for MA (no cement) and MAC1 (1% AC).

The results obtained in this work validate the particle size optimization carried out using the DoE methodology for simultaneous fresh paste high flowabilty and post-sintering performance, of which mixture MA is the final result. The adequacy of the FI test, in all its simplicity, to characterize the flowability behaviour of these materials and of the use of FI test results in the calculation of the corresponding property mathematical models and response surfaces is, thus, demonstrated.

These results are an important contribution to related previous work [7], which showed that, although the presence of calcium aluminate cement improves the dried mechanical strength (easier demoulding and handling), the properties of the sintered all-alumina self-flow castable (MA), particularly at high temperature and under thermal cycling, are generally better.

Acknowledgements

Funding from the Portuguese Foundation for Science and Technology (FCT, Project: PTDC/CTM/66302/2006) is gratefully acknowledged.

References

[1] L.P. Krietz, R.E. Fisher, J.G. Beetz, Evolution and status of refractory castable technology entering the 1990s, American Ceramic Society Bulletin 69 (1990) 1690–1693.
[2] W.E. Lee, R.E. Moore, Evolution of in situ refractories in the 20th century, Journal of the American Ceramic Society 81 (1998) 1385–1410.
[3] R.G. Pileggi, A.R. Studart, M.D. Innocentini, V.C. Pandolfelli, High-performance refractory castables, American Ceramic Society Bulletin 81 (2002) 37–42.
[4] S. Goberis, I. Pundene, The medium-cement refractory castable — a promising material for thermal power units, Refractories and Industrial Ceramics 43 (2002) 306–309.
[5] Y.E. Pivinskii, O.G. Us'yarov, A new generation of unshaped refractories, Refractories and Industrial Ceramics 47 (2006) 30–35.
[6] A.P. Silva, D.G. Pinto, A.M. Segadães, T.C. Devezas, Designing particle sizing and packing for flowability and sintered mechanical strength, Journal of the European Ceramic Society 30 (2010) 2955–2962.
[7] D.G. Pinto, A.P. Silva, A.M. Segadães, T.C. Devezas, Thermomechanical evaluation of self-flowing refractory castables with and without the addition of aluminate cement, Ceramics International 38 (2012) 3483–3488.
[8] A.P. Silva, A.M. Segadães, T.C. Devezas, Statistical modelling of the particle size composition of an alumina matrix for no-cement self-flowing refractory castables, Materials Science Forum 514–516 (2006) 604–608.
[9] A.P. Silva, A.M. Segadães, T.C. Devezas, MPT influence on the rheological behaviour of self-flow refractory castables, Materials Science Forum 587–588 (2008) 133–137.
[10] A.P. Silva, T.C. Devezas, A.M. Segadães, Effect of fine matrix content and coarse aggregate particle size on the final properties of self-flow no-cement refractory castables, in: German Refractories Association (Eds.), Proceedings of UNITECR'07, Dresden, Germany, 2007, pp. 524–527.
[11] T. Zhang, Q. Yu, J. Wei, P. Zhang, P. Chen, A gap-graded particle size distribution for blended cements: analytical approach and experimental validation, Powder Technology 214 (2011) 259–268.
[12] R. Myers, D. Montgomery, Response Surface Methodology, John Wiley and Sons, New York, 2002.
[13] J. Cornell, Experiments with Mixtures, John Wiley and Sons, New York, 2002.
[14] D.G. Pinto, A.P. Silva, A.M. Segadães, T.C. Devezas, Influence of surface area in the flowability behaviour of self-flow refractory castables, Materials Science Forum 636–637 (2010) 124–129.
[15] C. Hu, F. Larrard, O.E. Gjørv, Rheological testing and modelling of fresh high performance concrete, Materials and Structures 28 (1995) 1–7.
[16] R.B. Bird, G.C. Dai, B.J. Yarusso, The rheology and flow of viscoplastic materials, Reviews in Chemical Engineering 1 (1982) 1–70.
[17] V. Petkova, V. Samichkov, Some influences on the thixotropy of composite slag Portland cement suspensions with secondary industrial waste, Construction and Building Materials 21 (2007) 1520–1527.
[18] L.A. Pereira de Oliveira, Rheology of mortars and self-compacting concrete: modelling, in: University of Beira Interior (Eds.), Proceedings of 5th Conference Engenharia'2009 — Innovation & Development, Covilhã, Portugal, 2009 (in Portuguese).
[19] A.P. Silva, Metodologia para a obtenção de betões refractários auto-escoantes sem cimento de 100% de alumina, Portuguese Patent 103432, February, 2008 (in Portuguese).